Development of a low cost pupillometer-eyetracker and applications

Arturo Bianchetti[a], Liliana I. Perez[b,c], Silvia A. Comastri[a,c]

[a]Grupo de Óptica y Visión, Dto. Física, Facultad de Ingeniería, Universidad de Buenos Aires, Av. P. Colón 850 (C1063ACV) CABA, Argentina; [b]Grupo de Láser, Óptica de Materiales y Aplicaciones Electromagnéticas, Dto. Física, Facultad de Ingeniería, Universidad de Buenos Aires, Av. P. Colón 850 (C1063ACV) CABA, Argentina; [c]Consejo Nacional de Investigaciones Científicas y Técnicas, Av. Rivadavia 1917 (C1033AAJ) CABA, Argentina

ABSTRACT

The determination of ocular pupil diameter and gaze direction is important in various psychophysical and cognitive tests and can be accomplished using commercial, academic or open-source devices. In this work we develop a table-top pupillometer eyetracker termed Blick, the hardware costs 50 dollars and the software is open source (https://github.com/abianchetti/blick). The hardware is mounted in a portable holder and comprises an illumination system (two infrared LEDs generating 0.13 W/m^2 at 22 cm) and a detection system (containing an USB camera, an infrared filter and a 16mm lens system) The software, programmed in C++ using OpenCV and cvblob libraries, processes eye images in real time and supplies plots and tables of pupil diameter and gaze direction and a video of the eye. As applications, capturing the right eye of six young emmetropes and after performing the pixel-mm and homographic calibrations (required to determine diameter in mm and gaze direction), we conduct three tests. The corresponding tasks are to detect mistakes in three series of four poker cards, to recognize letters F between distractors and to write a sentence via eye movements using Blick as eye tracker and the tool Dasher (MacKays´s Cambridge Group). We obtain that Blick´s performance is satisfactory (errors being 0.05 mm in pupil diameter and 1 degree in gaze direction); that there are slight pupil dilations when subjects used to playing cards find mistakes and when some subjects find targets and, finally, that Blick can be employed as eyetracker to allow communication of disabled persons.

Keywords: pupillometer, eye tracker, cognitive tests, physical disabilities.

1. INTRODUCTION

The visual system comprises the ocular and neuro-retinal systems[1] and, composing it, the pupil is governed by the autonomic system, respectively contracting and dilating with parasympathetic and sympathetic activities[2]. If external conditions (illumination, contrast, stimulus location, etc.) are maintained constant, the pupil of a human being may dilate when he sees something attracting his attention and contracts if his eye accommodates. The pupil plays a main role in visual quality since it affects the amount of light entering the eye, retinal illumination, diffraction, threshold frequency of the contrast sensitivity function, aberrations, focal depth, etc.[3,4,5]. Either for a natural or artificial pupil, visual performance for a certain pupil size is evaluated using both objective tests (determination of corneal[6,7] or ocular[8,9,10] aberrations; evaluation of the ocular PSF and MTF[11]; etc.) and psychophysical tests (visual acuity[12]; contrast sensitivity[13,14]; brightness or sinusoidal patterns perception under glare conditions[15]; etc.). Additionally, changes in pupil size reflect brain activities such as emotions[16] (fear, disgust, etc.), cognitive load[17,18] (appearing when a subject is overwhelmed, stressed or doing a great mental effort to accomplish a task) or various interests such as sexual[19,20,21]. Brain activity can be determined by means of the non-invasive method of measuring pupil dilation[22] as well as using techniques such as electroencephalography, magneto encephalography, functional magnetic resonance and positron emission tomography[23]. Some of the tests traditionally employed to determine cognitive load using pupillometry are mental solving of mathematical operations[24], memorization of digits sequences[25], evaluation of a person's state of alert[26], etc. Pupillometry is employed, in adults, children and babies, in Ophthalmology, Social and Clinical Psychology, Neurology, Marketing, Sports and Physiological Optics. In the latter, a device measuring ocular pupil diameter is termed pupillometer and that determining gaze direction is termed eyetracker. In tests determining visual performance it is usually of greater interest to know pupil diameter than gaze direction[27] whereas human-computer interfaces only require

the determination of gaze direction[23]. Nowadays, commercial pupillometers-eyetrackers are usually integrated in one device often termed "eyetracker" (Tobii, Neuroptics, Arrington, etc.) costing around U$S 10000 while open source eyetrackers[28] (Opengazer, ITU Gaze Tracker, etc.) are mainly designed to determine gaze direction alone.

In this work, based in Bianchetti´s Thesis[29,] we develop a pupillometer-eyetracker, termed Blick, and we show some applications. Blick is a table-top device designed to optimize iris-pupil contrast, it comprises a low cost hardware (U$S 50) and an open source software (https://github.com/abianchetti/blick) and it determines ocular pupil diameter and gaze direction in real time with reasonable precision. In Section 2 we describe concepts related to the hardware of Blick, composed by a detection system (consisting in a conventional USB camera of domestic use, a lens system and a filter blocking visible radiation) and an illumination system (consisting in two infrared LEDs regulated in intensity by a variable resistor). In Section 3 we briefly explain the image processing techniques employed by the software of Blick (implemented in C++ using OpenCV and cvblob libraries); how to use Blick and the graphic user interface which enables parameters adjustment to optimize pupil detection, homographic calibration for eye tracking (using the first Purkinje images of both LEDs), pixel-mm calibration to measure real pupil diameter, generation of a pupil diameter plot and data storage. In Section 4, considering 6 young subjects, we show results obtained in the homographic calibration, in 2 tests (error recognition and target searching) designed taking into account other authors works[2,17,18] and, finally, in the task of writing a sentence in the computer via eye movements and using the tool Dasher[30] as interpreter.

2. HARDWARE OF BLICK

The hardware, termed SID (System Illumination-Detection), is composed by a detection and an illumination systems. In our tests (Figure 1), the SID is near the chin-rest where the subject places his chin and forehead and it is mounted on a support of adjustable height with a mobile head (which allow its positioning to adequately capture the eye).
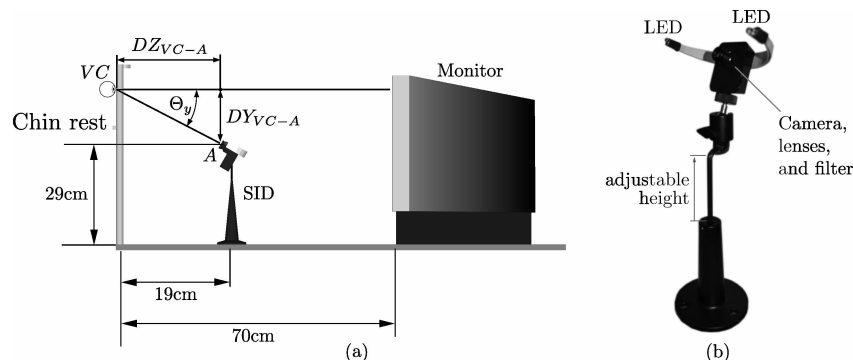

Figure 1. (a) Lateral set-up view: corneal vertex (VC), chin-rest, SID, sensor central point (A), distances DZ_{VC-A} and DY_{VC-A} (DX_{VC-A} perpendicular to figure), angle between the horizontal and the line $VC-A$ (Θ_y), monitor. (b) Photograph of the SID.

2.1 Detection system.

We design and build the detection system in such a way that it fulfills the following requirements.

(a) Adequate frame rate: The number of frames per second acquired enables precision of pupil variation measurements.

(b) Adequate resolution: We take into account that the precision of pupil diameter determination increases if, in the image captured by the camera, the number of pixels corresponding to the pupil increases.

(c) Sensitivity only to near infrared radiation: We use near infrared radiation (NIR) because this radiation (wavelengths between 760 and 1400 nm) can yield a larger iris-pupil contrast than light (wavelengths between 400 and 750 nm) and enables a pupil detection which is independent of the subject´s iris color and of ambient illumination conditions.

(d) Optical system of adequate power: The optical system power allows us to focus an eye located at a distance such that our table top device causes no discomfort to the subject and we choose this distance equal to approximately 20 cm.

(e) Low cost: Blick´s low cost allows many people (scientists, psychologists, disabled persons, etc.) to afford and use it.

We achieve these requirements composing the detection system of a modified camera, a lens system and an infrared filter. We choose the camera taking into account that commercially available USB cameras usually contain a CCD or CMOS sensor and a system of lenses and filters, those for scientific use (Optitrack V120:SLIM, Im. Source DFK21AF04AS, Iva 2MUSB-7.5HRLL, Hitachi KP-F31SCL, etc.) costing around 300 to 600 U$S while those for domestic use (Phillips SPC530; Sony PS Eye, etc.) costing around 30 U$S. The latter can present limitations if used to determine gaze direction in real time since they often have an automatic exposure control (various frames are superposed pixel to pixel to increase the compound frame intensity thus yielding a small and variable frame rate) and a filter that blocks infrared radiation (transmitting only light and hence reducing the iris-pupil contrast). The control can seldom be annulled and the filter is adhered to the sensor or lenses and can sometimes be removed. The camera we employ is the Philips SPC530, it is of domestic use and low cost (verifying requirement (e)); it enables the annulment of the automatic exposure control (thus fulfilling requirement (a) and frame rate being up to 30 fps) and it contains a CMOS sensor sensitive to visible and infrared radiations and a filter blocking infrared which can be easily removed. Furthermore, this camera originally contains a wide angle lens system and the sensor should be less than 5 cm apart from the eye to capture adequate ocular images. To avoid subject´s discomfort and satisfy requirements (b) and (d), we replace this lens system by another without filter, of 16 mm focal length and such that, via manual focusing, it allows ocular images capture with 640×480 pixels resolution in a range of distances between approximately 15 and 25 cm. To verify requirement (c), we use a filter that blocks light and transmits NIR. In Figure 2, in (a) we depict the eye, the lens system (represented by its principal planes Π and Π' whose location we ignore and with focal points F and F'), the filter that blocks light and the sensor and in (b) we show a photograph of the lens system and the filter adhered to its internal face.
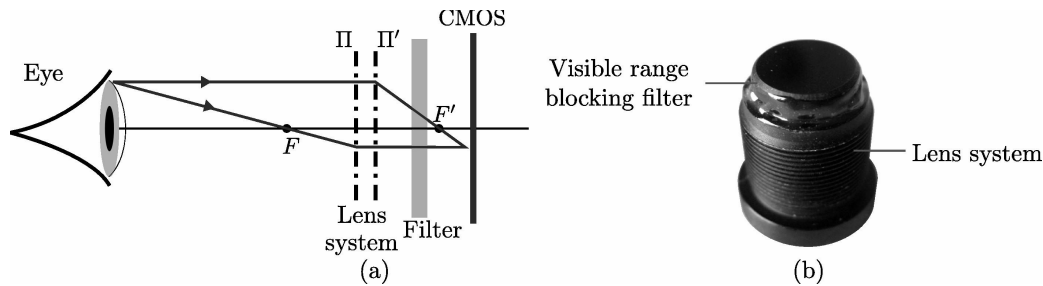

Figure 2. (a) Diagram of the eye, lens system, filter and CMOS sensor. (b) Photograph of lens system with filter adhered.

2.2 Illumination system

The illumination system verifies the following requirements.

(f) Illumination in the NIR range: Radiation within the NIR range allows the detection system to work under photopic, mesopic and scotopic conditions and, because of their voltage and consumption characteristics, we choose LED sources.

(g) Adequate pupil-iris contrast: We choose the LEDs location so as to attain pupil radiance lower than that of the iris.

(h) Cuasi-uniform radiation pattern at the eye: We radiate the eye almost uniformly to avoid local variations of contrast.

(i) Not obstructed visual field: We choose a LEDs array that does not obstruct the subject´s visual field.

(j) Adequate first Purkinje images location: We choose a LEDs images array that simplifies the eye tracking algorithm.

(k) Irradiance at the eye lower than the limit for safe measurements: According to ICNIRP (International Commission on Non-Ionizing Radiation Protection), ocular exposure must not exceed 100 W/m^2 for exposures longer than 1000 s.

To verify requirement (f) and after trying various wavelengths, we irradiate with LEDs of 850 nm. If the LEDs are placed near the lenses optical axis (Figure 3 (a)), radiation incident on the retina is partially reflected towards the camera causing the pupil to be brighter than the iris[17] whereas if the LEDs are laterally located (Figure 3 (b)), it is possible to avoid this reflected radiation and, in this case, the pupil is darker than the iris. We place the LEDs in such a way that the latter and requirement (g) are verified. Moreover, the radiation pattern at the eye depends on the quantity and location of the LEDs and, after trying various symmetric configurations, we decided to use two LEDs such that a=6 cm in Figure 3

(b) and requirements (h), (i) and (j) are fulfilled. Concerning requirement (k), we minimize the risk of causing ocular damages (especially during the device trial period), including an intensity regulator (variable resistor) which allows attenuation. If the LEDs are 22 cm apart from the eye, the measured maximum irradiance at the cornea is 0.126 W/m^2 which is much smaller than the ICNIRP limits for the exposure times used in our tests (lesser than 1000 s).
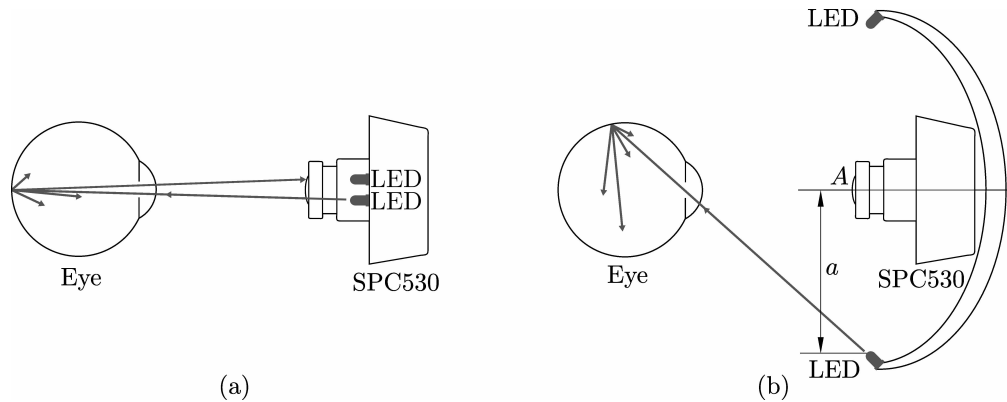

Figure 3. Possible locations of LEDs generating NIR that is incident at an eye (for simplicity we leave aside refraction at the crystalline lens). (a) LEDs near the lenses optical axis. (b) LEDs displaced from the lenses optical axis.

3. SOFTWARE OF BLICK

The software is implemented in C++ using OpenCV and cvblob libraries, it can be used in a personal computer running Linux, it comprises the processing and segmentation of pupil and Purkinje images and it has a graphic user interface.

3.1 Processing and segmentation of pupil images

Pupil image processing (Figure 4 upwards) reduces the amount of useless information present in the captured image, optimizes and accelerates the subsequent segmentation processes and is carried out in the 4 following steps.

• **Grey scale conversion:** We capture frames at a rate of at most 30 fps and with resolution of 640 x 480 pixels. The image in each frame is in RGB mode and we convert it to grey scale using cvCvtColor of the OpenCV library[31].

• **Histogram equalization:** To equalize the histogram representing the grey level distribution, we expand the dynamic range in the image and optimize the perceived pupil-iris contrast using cvEqualizeHist of OpenCV[31].

• **Blurring:** We reduce noise employing spatial filtering with Gaussian masks by the use of cvSmooth of OpenCV[31].

• **Thresholding:** In the original image there can be 256 grey levels and, to simplify segmentation and using cvThreshold of OpenCV[31], we reduce this number to two, grey levels lower than T_{pupil} are transformed to 255 (white) while those greater than T_{pupil} become 0 (black), T_{pupil} being a threshold chosen by the user and equal to 10 by default.

As a result of the processing stage, the image is binary and, ideally, contains information concerning the pupil, eyebrows, eyelids and nearby shadows. On the other hand, image segmentation (Figure 4 downwards) allows us to separate and measure the pupil and is carried out in the 4 following steps.

• **Blobs labeling:** To distinguish each object or blob from another, we mark each one with a label. To do so we scan the image from left to right and from top to bottom and, taking into account that two pixels are connected[32] if they are neighbors and have the same grey level, we assign a label to each blob using a method that does not require re-labeling implemented in the cvblob library[33].

- **Area filtering:** Counting the amount of pixels with a certain label, we determine each blob area, S, and filter blobs whose size cannot correspond to a pupil, this size being defined by the user employing the parameters S_{Pmin} and S_{Pmax} (minimum and maximum pupil areas) which respectively are 2000 and 15000 pixels^2 by default.

- P**olygon pupil approximation:** Excluding abnormal pupils such as those with colobom, pupil area is often apparently smaller than the real one because of reflections or noise and we avoid the consequent measurement errors approximating the pupil to a simple convex polygon. To do so we use Melkman´s algorithm[34] implemented in the cvblob library[33].

- **Circularity filtering:** Leaving aside ocular pathologies, pupils of normal eyes are usually nearly circular so, to distinguish a pupil of perimeter p and area S from other blobs, we define circularity as $c_{Blick}=100-10\,((p^2/S)-4\pi)$ adapting the formula $c_{cvblob}=(p^2/S)-4\pi$ of the cvblob library[33] so that the maximum value of c_{Blick} is 100.

As a result of segmentation, the ocular image contains the detected pupil with its contour indicated by a red polygon (marked light grey en Figure 4). We evaluate pupil diameter measured in pixels, termed DP_{pixels}, calculating this polygon area, S_P, and assigning it to a circle of area $(\pi/4)(DP_{pixels})^2$, this is, we have $DP_{pixels}=(4\,S_P/\pi)^{1/2}$.
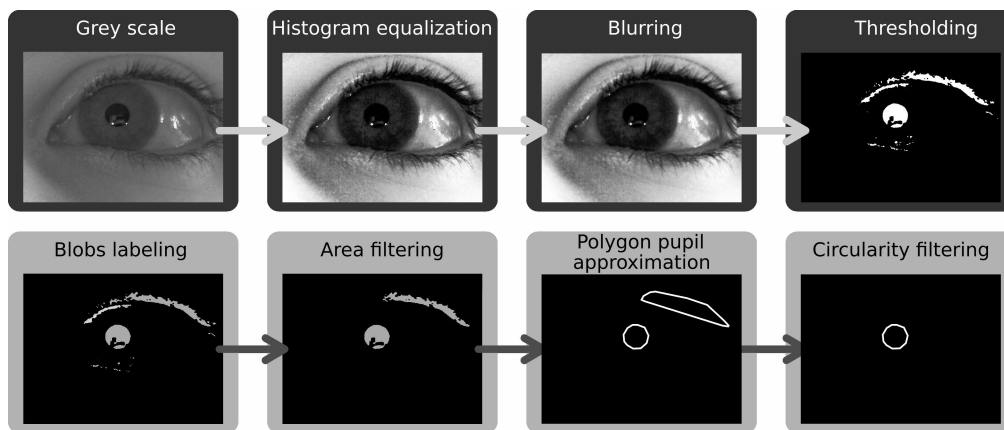

Figure 4. Software of Blick: pupil image processing (upwards) and segmentation (downwards).

3.2 Processing and segmentation of Purkinje images, homographic calibration and eye tracking

The detection of the first Purkinje images (which are the images of light sources by reflection in the external corneal face) allows us to determine gaze direction. In normal eyes, the external corneal face is approximately spherical so, when the eye rotates, the first Purkinje images remain almost stable while the pupil center rotates. In Blick, these images correspond to both LEDs present in the SID and, to detect them, we use a proceeding similar to that described in Section 3.1 for the pupil though with different parameters. The threshold, $T_{Purkinje}$, is such that grey levels greater than $T_{Purkinje}$ are transformed to 255 (white) while those lower than $T_{Purkinje}$ become 0 (black), $T_{Purkinje}$ being chosen by the user and equal to 235 by default. The minimum and maximum areas used to filter blobs, S_{Rmin} and S_{Rmax}, are chosen by the user and are respectively 10 and 200 pixels^2 by default. To acquire and process Purkinje images avoiding misleading reflections, we take into account only a portion of the whole captured ocular image defining a region of interest (ROI) of 300 x 200 pixels centered in the pupil centre (Figure 5).
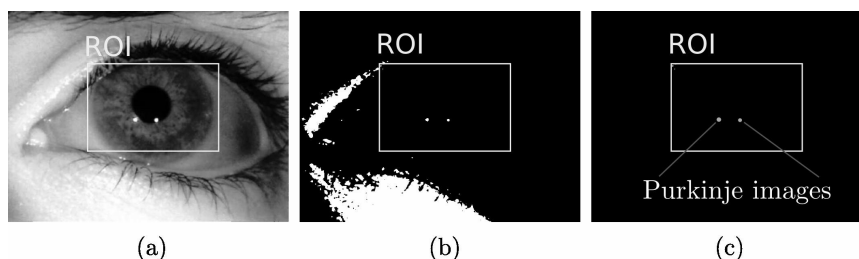

(a)   (b)   (c)

Figure 5. First Purkinje images detection. (a) Region of interest (ROI). (b) Image after thresholding. (c) Final image.

After detecting the Purkinje images, Blick calculates the medium point between them, *IP*, and the line joining *IP* and the pupil center, *CP*. The user must check that the pupil image centre lies in the sensor when the subject looks at any contour point of the monitor or screen where the stimuli appear and the line *CP-IP* varies when gaze direction varies. For instance, when an eye looks at points *UL*, *UR*, *DL* and *DR* placed in the corners of a rectangular monitor and at its central point, *CT*, the line *CP-IP* varies as in Figure 6 (a). If UL_O, UR_O, DL_O and DR_O denote the images of *CP* at the SID sensor when the subject looks at *UL*, *UR*, *DL* and *DR* respectively, the polygon with vertexes at UL_O, UR_O, DL_O and DR_O is usually a distorted rectangle because the direction *VC-A* is neither horizontal nor vertical (Figure 1), the lens system constituting the SID has aberrations, etc.
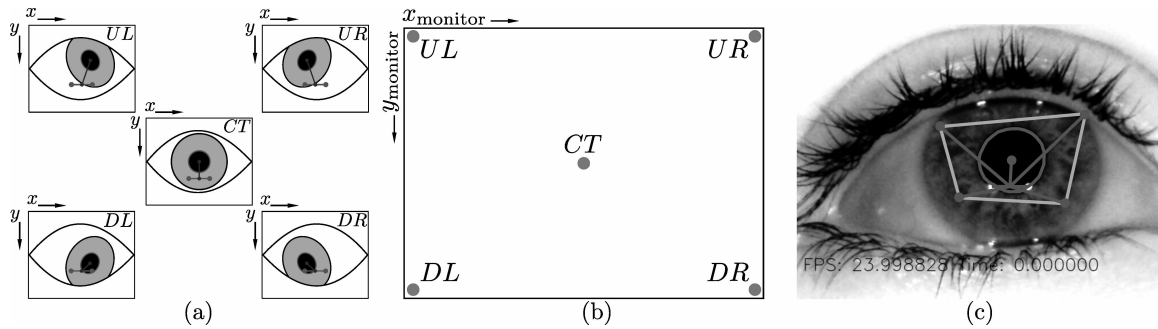

Figure 6. Gaze direction. (a) Variation of the line *CP-IP* when gaze direction varies (*CP*: pupil centre, *IP*: medium point between Purkinje images). (b) Monitor points *UL*, *UR*, *DL*, *DR* and *CT*. (c) Polygon when viewing points *UL*, *UR*, *DL*, *DR*.

To take into account the above mentioned distortion when determining gaze direction, a calibration is required and, considering (as occurs in this paper) that the stimuli are shown in a monitor, in its plane we define coordinates ($x_{monitor}$, $y_{monitor}$) and an arbitrary viewed point, *Q*, defined by the position vector, $\boldsymbol{\rho}$ (Figure 6 (b)). Correspondingly, in the sensor we consider a position vector, $\boldsymbol{\rho}'$, from *IP* to the pupil center when the subject looks at *Q* (Figure 6 (c)). If κ is a constant factor, *H* is a matrix transforming vectors $\boldsymbol{\rho}$ into $\boldsymbol{\rho}'$ and (i) denotes each vector taken into account (i=1, 2,…), we have $\boldsymbol{\rho}'^{(i)} = \kappa H \boldsymbol{\rho}^{(i)}$. In Blick this transformation is performed using the function cvFindHomography which is such that the vectors $\boldsymbol{\rho}$ and $\boldsymbol{\rho}'$ are the entrance data and *H* is the homographic transformation matrix. To determine $\boldsymbol{\rho}^{(i)}$ and $\boldsymbol{\rho}'^{(i)}$, the subject must perform an homographic calibration looking at 25 monitor points ($Q^{(i)}$) centered at argentine cockades (the complete calibration board is that of Figure 7 (a) though the subject sees one cockade at a time as in Figure 7 (b)). When a subject looks at a point $Q^{(i)}$, Blick determines $\boldsymbol{\rho}^{(i)}$ and $\boldsymbol{\rho}'^{(i)}$ and recalculates *H* and, during the whole process, calibration can be controlled in real time since the estimated gaze direction is towards the center of a marked grey circle (for example in Figure 7 (a) the subject would be looking at the central cockade). If the number of points $Q^{(i)}$ increases, theoretically, the calibration precision would increase but, in practice, the subject´s fatigue might also increase worsening the results and, as we show in the following Section, 25 turns out to be an adequate number. When calibration ends, the matrix *H* is known so, for a measured value of $\boldsymbol{\rho}'^{(i)}$, Blick determines $\boldsymbol{\rho}^{(i)}$ thus enabling eye tracking.
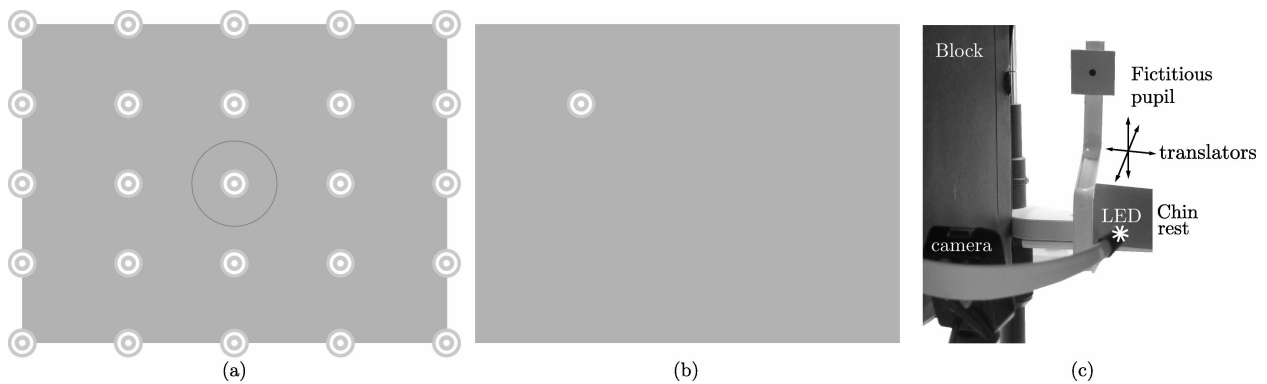

Figure 7. (a) Homographic calibration board containing 25 argentine cockades (white and light blue concentric circles). (b) Calibration image with one cockade shown to the subject. (c) Pixel-mm calibration using a fictitious pupil of diameter 5mm.

3.3 Pixel-mm calibration to measure real pupil diameter

To adequately measure pupil diameter in millimeters, termed DP, we detect a fictitious pupil (Figure 7 (c)) of diameter 5mm whose diameter measured in pixels is $DP_{fictitious}$ when placed in the location of each subject´s pupil. We have $DP = $ 5mm (DP_{pixels} / $DP_{fictitious}$). Furthermore, by the use of Gnuplot Pipes[35], Blick can plot DP versus time in real time.

3.4 Graphic user interface and use of Blick

The graphic user interface (GUI) contains a terminal for data entry (subject's name and age, comments and instructions to capture from file or camera and to save video file or not); windows showing images useful to verify adequate detections entitled "Pupil tracking" (detected pupil image), "Gnuplot" (plot of pupil diameter vs time), "Threshold pupil image" and "Threshold Purkinje image" and settings to adjust parameters optimizing pupil detection for the existing external conditions and command the beginning of processes (Figure 8). These settings are: pupil and Purkinje thresholds, (T_{pupil} and $T_{Purkinje}$); minimum and maximum pupil areas in pixels (S_{Pmin} and S_{Pmax}); minimum and maximum Purkinje areas (S_{Rmin} and S_{Rmax}); pupil circularity (c_{Blick}); a "record" bar to start data storing, a "calibrate" bar to start homographic calibration, a "track" bar to start eye tracking; a "plot" bar to start plotting pupil diameter vs time and a "píxel-mm calibrate" bar to perform pixel-mm calibration. Moreover, when capturing, the user can mark data of interest employing a parameter (termed *Tag*) such that *Tag*=0 (default) or *Tag*=1 (for data of interest). It is interesting to point out that Blick detects the subject´s blinks, shows the word "Blink" in the window "Pupil Tracking" and stores neither pupil diameter nor gaze direction data during blinking.
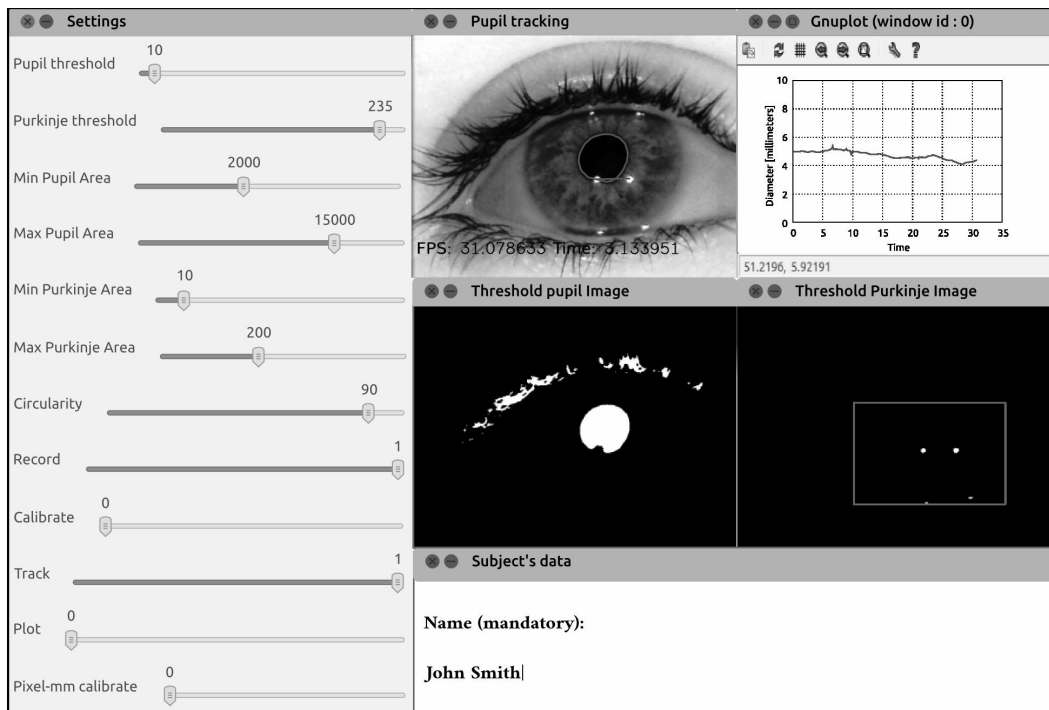

Figure 8. GUI: settings (to the left); detected pupil and diameter plot (upwards to the right); threshold pupil and Purkinje images (center to the right); terminal to enter data, e.g. subject´s data, capturing information, etc. (downwards to the right).

To adequately employ Blick, the user must carry out the following 4 steps.

I. Enter subject´s and modality data: The user must complete data appearing in the terminal entitled "subject´s data" in Figure 8. He must first complete the subject´s data which are name (mandatory), age (optional) and comments (optional). When a subject´s name is entered for the first time, a folder with this name, the date and the hour is automatically created whereas if a subject´s name previously considered is entered, the data are stored in his folder but the date/hour of files differs from the earlier ones so files are not overwritten. Concerning entrance data, the user must

specify whether he wants to employ text data previously stored in a folder (specifying its name) or a video stored earlier (placing this file in the same directory as Blick and specifying its name with extension .avi) or to capture new pupil data using the SID. Regarding exit data, by default, Blick stores the capturing time, DP, $x_{monitor}$, $y_{monitor}$ and information concerning tagged data and homographic calibration and, optionally, Blick can save the video file containing the frames of the rendered pupil (with its contour outlined in red) and Purkinje images, the number of fps, etc.

II. Set parameters and calibrations: The user must set the parameters appearing in the window "Settings" of the GUI. He can either adjust parameters T_{pupil}, $T_{Purkinje}$, S_{Pmin}, S_{Pmax}, S_{Rmin}, S_{Rmax} and c_{Blick} or accept the default values. Moreover, to measure pupil diameter in millimeters, sliding the bar "Pixel-mm calibrate" to the right for some seconds and then to the left to start capturing and adjusting parameters if necessary, the user must capture during about 10 s a 5 mm fictitious pupil placed in the location of each subject´s pupil. To determine gaze direction, the user must slide the bar "Track" towards the right, verify that Purkinje images are adequately detected and perform the homographic calibration sliding the bar "Calibrate" towards the right. The subject sees one cockade at a time as in Figure 7 (b) and must be instructed to look at it continuously. In the meantime, the user must control this point calibration verifying that the grey circle and the cockade centers coincide (he must press the key "m" for the subject to start moving the pointer with his eyes and the key "n" to end). When the user considers the information is adequate enough to be stored, he must press his computer space bar (this causing the cockade centre to become yellow) and, then, employing the arrow keys, he must present another cockade. The procedure must be repeated for the 25 points and the calibration mode ends pressing the backspace key.

III. Capture and store data: While capturing images, the user can optionally start storing data in the subject´s folder (sliding the bar "Record" towards the right); re-adjust parameters in real time (T_{pupil}, $T_{Purkinje}$, etc.); mark ranges of data of interest (pressing the key "s", *Tag* becomes equal to 1 and the word "Tag" appears in the "Pupil tracking" window while pressing the key "e", *Tag* returns to the value 0); plot pupil diameter in real time (sliding the bar "Plot" towards the right) and end capturing (sliding the bar "Record" towards the left and closing the window "Settings").

IV. Process exit data: When the storage stage ends, the user disposes of information which he can process according to his needs. This information can be: subject´s name and age, comments and measurement date (in datafile.dat); data in text format which is time, pupil diameter, $x_{monitor}$, $y_{monitor}$ and *Tag* (in the file captureData.dmt which can be employed to plot DP, $x_{monitor}$ and $y_{monitor}$ vs time); homographic calibration data (in the file calibration.xml) and rendered video with pupil contour outlined in red, Purkinje images joined by a blue line, number of fps, capture time, etc. (in a .avi file).

4. EXPERIMENTAL SETUP, METHODOLOGY, TASKS, SUBJECTS, RESULTS

Each of the six considered subjects performs the pixel-mm and homographic calibrations; two tests[17,18] (in the first he must recognize mistakes in a sequence of 4 poker cards, 2 mistaken, and in the second he must find letters F placed between distracters) and, finally, he writes a sentence via eye movements using Blick as eyetracker and the tool Dasher[30] as interpreter. In Figure 9 we represent time sequences, in (a) for all the tests and in (b) for the cards test in particular.
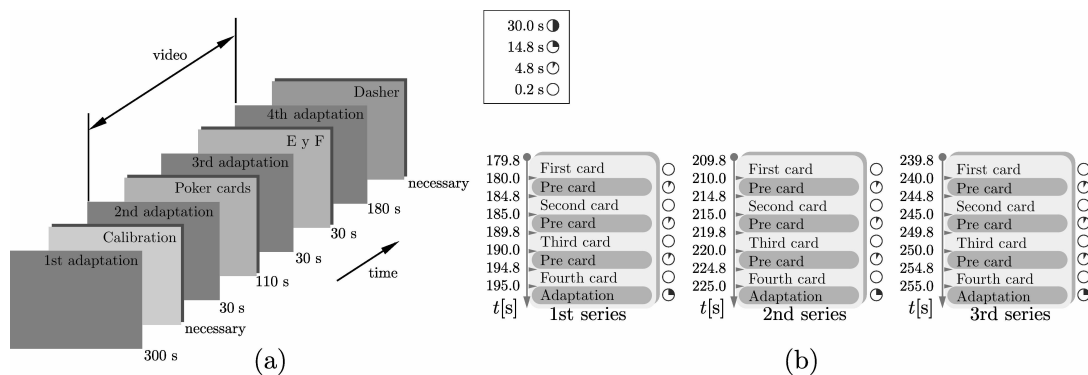

Figure 9. Time sequence. (a) All the tasks and adaptations: homographic calibration, poker cards, letters F, writing in PC via eye movements. (b) Poker cards test: three series of the same four cards, each preceded by the adaptation/rest image.

4.1 Experimental setup

The experimental setup is mounted on a table 200 cm long and 80 cm wide with a dark grey rubber cover and placed in a yellow room (5.7 m long and 3.6 m wide) with windows blocked out by black cardboards. The setup consists in a monitor ViewSonic E70FSB of 17"; the SID; a laptop; a device termed Block; a fictitious pupil and the radiation sources (Figure 10 (a) and (b)). The tests are shown in the monitor placed on a support 12 cm high and 70 cm apart from the subject´s eye, its border is not masked (for conditions to be similar to those which could be encountered in other research laboratories, ophthalmologic or psychological rooms, etc.) and its visual field is 24.7° horizontally and 19.1° vertically. The SID contains the two LEDs, the system lenses-filter-detector and a height regulator that can also rotate in an axis perpendicular to the table to enable adequate capture for each subject and, during our tests, the SID´s location is that of Figure 10 (a), VC-A=20.4 cm and $\Theta_y \approx 20.2°$ (Figure 1 (a)). In the laptop we use Blick´s software to process the information captured by the SID. The Block consists in a chin-rest of fixed height relative to the table and a partial occluder (that facilitates illumination control and reduces possible subject´s distractions). The 5 mm fictitious pupil is mounted in three positioners along the horizontal, vertical and longitudinal axes which allow us to place it in the location of each eye for an adequate pixel-mm calibration. Besides the LEDs and monitor, the sources are 12 fluorescent tubes (each of 36 W) placed in the ceiling (175 cm apart from the table) so the illumination is photopic. If $L_{stimulus}$ and $L_{surrounding}$ are the luminances (measured with a luminancimeter LMT L 1003) at the monitor and at its surroundings, we have $L_{stimulus}$ equal to 39.0 cd/m^2 in the homographic calibration, 37.3 cd/m^2 in both tests and 91.0 cd/m^2 in the Dasher image and, considering an average of luminances measured along the monitor border, $L_{surrounding}$=55 cd/m^2 in every case.
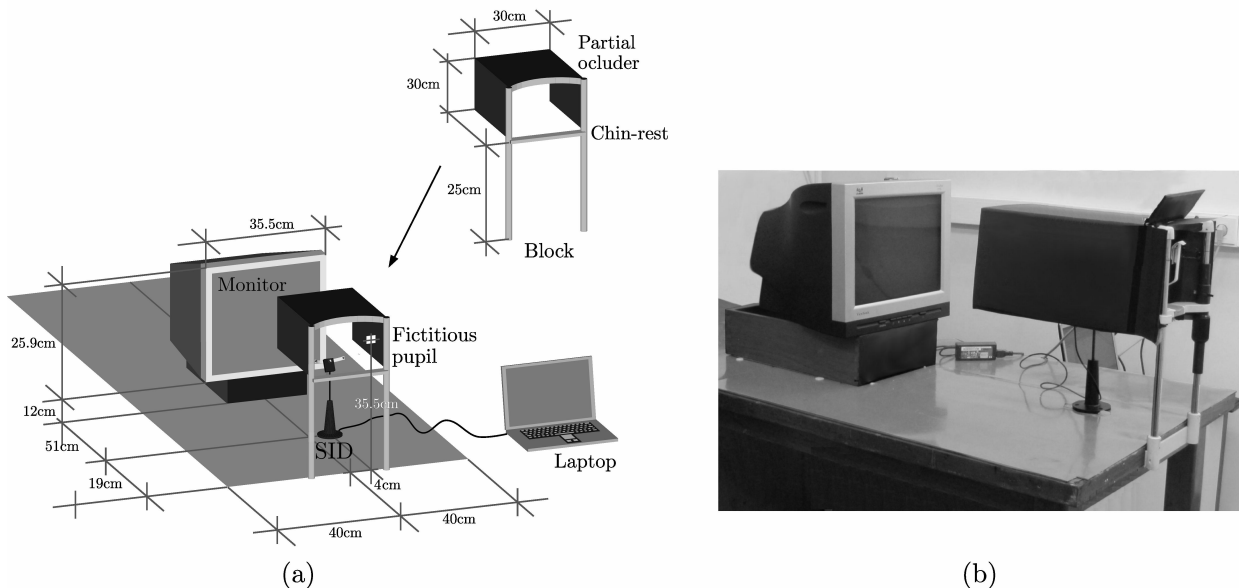

Figure 10. Experimental setup. (a) Diagram indicating distances. (b) Photograph.

4.2 Methodology and tasks

During the experiment, the subject is seated placing chin and forehead on the chin-rest and, for this to be comfortable, we adjust his seat height. The subject performs the tasks binocularly but we only detect the pupil of his right eye. At the beginning of each session, the subject performs the pixel-mm calibration. Moreover, before each task and to adapt to the illumination and rest a little, the subject looks at an adaptation/rest image of luminance and color similar to that of the oncoming image. The whole session contains the following four tasks.

• **Homographic calibration:** While the subject looks at the adaptation/rest image (Figure 8 (b)) during 300 s, he answers a questionnaire (name, age, nationality, health state, use of contact or ophthalmic lenses, eye color, education degrees, number of hours per day using a computer, occupation, habits, hobbies, preferences, etc.) and, also, we briefly explain the tasks he is going to perform. As mentioned in Section 3.2, during the homographic calibration, the cockade occupies only one position at a time (as in Figure 8 (b)) and, when that point is recorded, the cockade moves to another

of the 25 possible positions (shown in Figure 8 (a)). The subject´s task is to look continuously at the centre of the presented cockade. On the other hand, to simplify the analysis of the calibration results, we draw density plots using the function SmoothScatterPlot of R with bandwidth=10 and we assign different colors or grey levels according to the points density (here we have light grey: moderately viewed zones; medium grey: most viewed; dark grey: less viewed).

• **First and second tests:** In the first and second tests (Figure 11 (a) and (b)) we respectively show 3 series of the same 4 poker cards (black characters on white background and cards "4" and "6" being incorrect) and a set of letters E with two rotated letters F among them (black characters on greenish background). Both tests are shown in a video consisting in a sequence of adaptation/rest images and tests and, to facilitate data processing, we tag the beginning and end of each test. The adaptation/rest images are similar to those of the tests to minimize differences in image quality, luminance, luminance contrast ($C=(L_O-L_B)/L_B$, L_O and L_B being the object and background luminances) and chromatic contrast between them. The subject´s task is to distinguish the incorrect cards in the first test and to find letters F in the second.
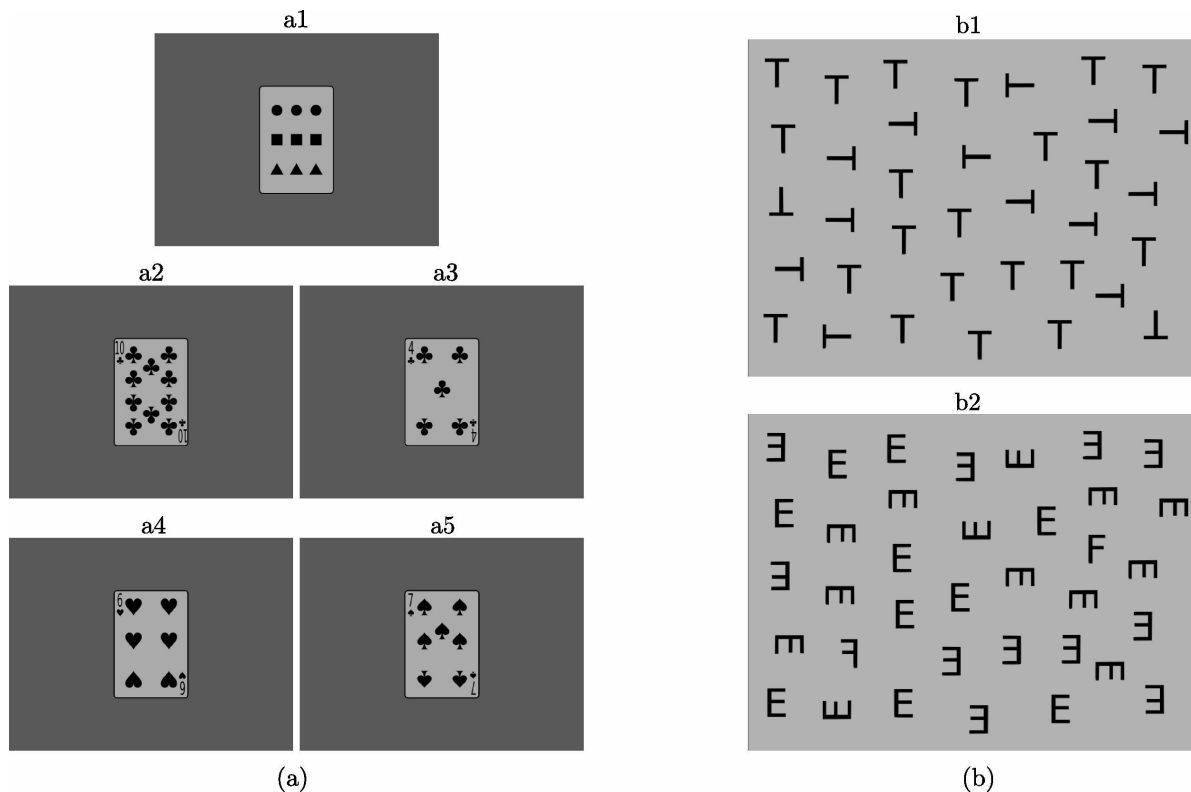

Figure 11. (a) First test (errors recognition): adaptation/rest image (a1); poker cards (a2-a5, a3 and a4 having errors). (b) Second test (search for letters F among distracters): adaptation/rest image (b1); letters F among letters E (b2).

• **Writing a sentence via eye movements**: The Dasher tool, of MacKay's Cambridge research group[30], enables the user to write text in a computer employing an eyetracker instead of a keyboard and, though it contains predictive text, in the present work we do not use it. Our adaptation/rest image is the graphic interface Dasher in static state (Figure 12), this adaptation lasts 180 s and, during it, we briefly explain to the subject how to write a word moving his eyes. For instance, in Figure 12, a subject wants to write the word "hola", he has already correctly written the first 3 letters and he is deviating the pointer towards the last letter, "a". Using Dasher and moving the pointer with his eyes by the use of Blick, each subject´s task is to write the sentence "me gusta viajar".
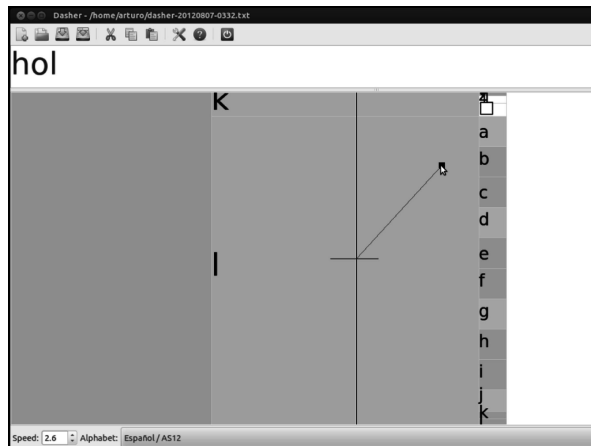
Figure 12. Writing a sentence via eye movements using the pupillometer-eytracker Blick and the tool Dasher.

4.3 Subjects

The subjects are 3 women (MM, AW, AM) and 3 men (HG, OM, PG), volunteers, young (mean age 33 years old), healthy, emmetropes (except AM with Sphere=-0.5 diopters and Cylinder=0) and working in the Instituto Nacional de Tecnología Industrial-Argentina. We do our best for each subject to be comfortable and calmed and none of them reports a serious uneasiness or fatigue though a few get temporarily distracted and move a little.

4.4 Results

Before analyzing the results, we estimate the errors in the determination of pupil diameter, ε_{DP}, and gaze direction, ε_{β}.
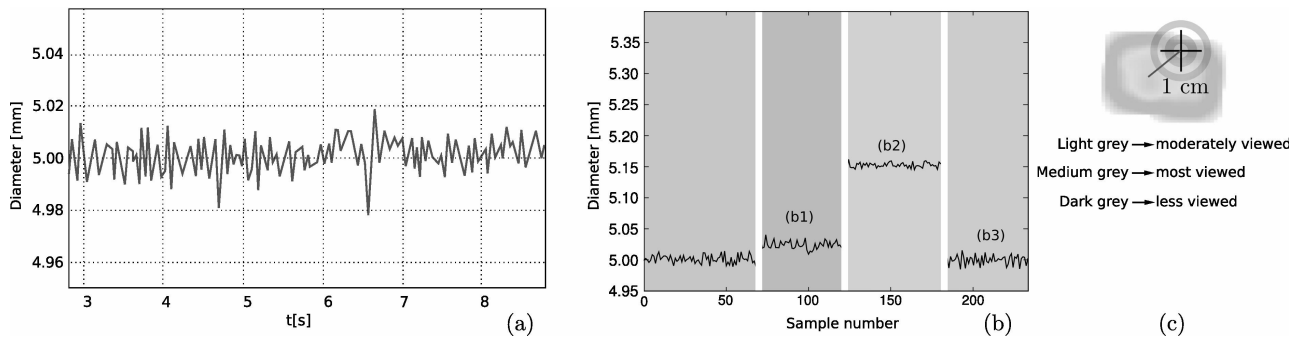

Figure 13: Errors. (a) Diameter of a 5 mm fictitious pupil. (b) Diameter for 2 cm displacements of the 5 mm pupil along the horizontal (b1), vertical (b2) and longitudinal (b3) directions.(c) Gaze direction: density plot and cockade center.

We estimate $\varepsilon_{DP} \approx 0.05$ mm taking into account that: i) the maximum difference with respect to the mean diameter detected for a 5 mm fictitious pupil is 0.02mm (Figure 13 (a)); ii) the subject´s eye could shift a little during the tests and, to try possible consequences of this, we displace in 2 cm (which is much larger than probable eye shifts) the 5 mm fictitious pupil and get that DP changes in 0.02 mm when varying DX_{VC-A}; in 0.15 mm when varying DY_{VC-A} and in a negligible value when varying DZ_{VC-A} (Figures 1 (a) and 13 (b)); iii) maintaining external conditions constant, the human pupil undergoes natural variations and in preliminary trials, detecting DP in the 6 subjects under photopic conditions, the minimum standard deviation resulted to be 0.04 mm. We estimate $\varepsilon_{\beta} \approx 1°$ taking into account the best homographic calibration (corresponding to subject PG) and, since the distance between the centers of the zone of greatest points density and of a cockade is 1 cm and the distance eye-monitor is 70 cm, we get arctan(1cm/70 cm)=0.82° (Figure 13 (c)).

● **Homographic calibration:** The calibration is satisfactory in most subjects and, as an example, in Figure 14 we show the results for subject PG. However, for subject AW, because of movements during and after the calibration, we have to adjust some parameters (particularly threshold) when we capture data, this affecting the eyetracking quality.
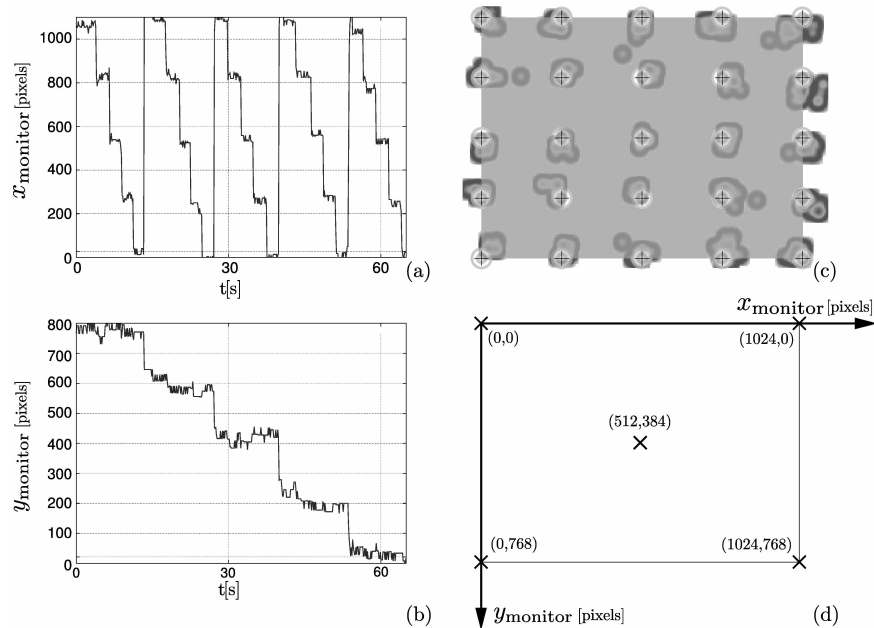

Figure 14: Homographic calibration of subject PG: (a) $x_{monitor}$ versus time. (b) $y_{monitor}$ versus time. (c) Density plot and crosses indicating the calibration cockades centers. (d) Characteristic points at the monitor.

● **Errors recognition in poker cards:** As mentioned above (Figure 11 (a)), there are 3 series of the same 4 cards (2 of them with errors), each being presented during 200 ms (Figure 9 (b)) and preceded by the adaptation/rest image. Only subjects MM and AM, who are the only ones who play with poker cards in daily life, find the errors. Moreover, following Klinger[17] (who averages many repeated measurements of the same task to reduce noise and/or other random dilations), we average the measurements of the 3 series (Figure 15 (a) and (b)) and evidence for AM alone, a slight pupil dilation (of approximately 0.2 mm) when each card appears and a very tiny additional dilation (approximately 0.05 mm) when the incorrect cards appear. This suggests that the probability of distinguishing errors in an image increases if the subject is habituated to this type of image and that, as mentioned by others[18], error recognition can be accompanied by slight dilations. However, to obtain more conclusive results, a larger number of series and subjects are required.
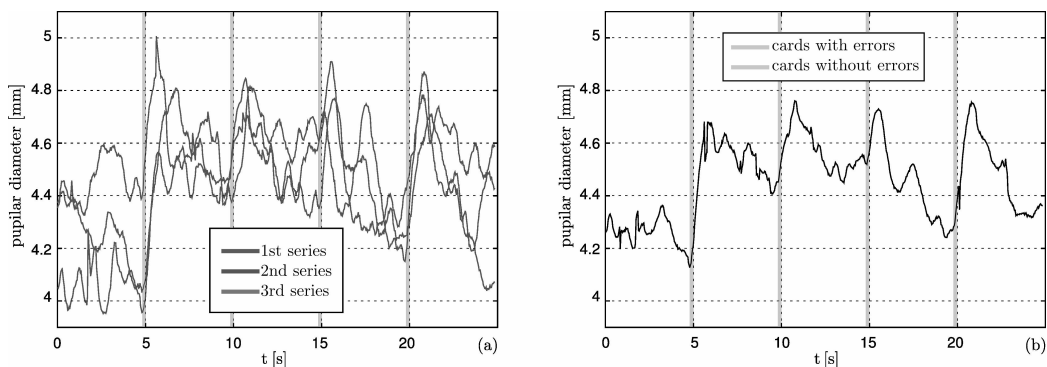

Figure 15: *DP* vs time for the poker card test of subject AM. (a) Three series of 4 cards. (b) Average of the 3 cards series.

● **Search for letters F among distracters:** The image is shown during a relatively long period (30 s) and all the subjects identify both letters F. In Figure 16 (a) we show gaze itinerary for subject PG when he identifies the letters F. To determine variations of pupil diameter, we calculate the difference between DP and the moving average of pupil diameter[36], DP_{WA}, and we obtain the plot of Figure 16 (b). When PG looks at the letters F, pupil dilatation results to be small and approximately equal to 0.04 mm, which is of the magnitude order of the measurement error and of results obtained by other authors[17]. For the other subjects, dilation is still smaller and, to obtain more conclusive results, a larger number of subjects and/or improvements in our methodology are required.
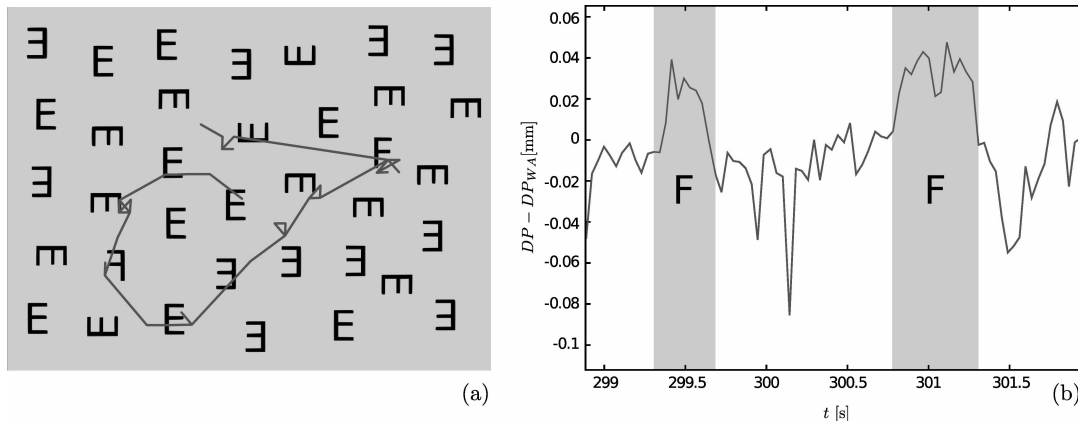

Figure 16: Search for letters F among letters E accomplished by subject PG. (a) Gaze itinerary. (b) DP-DP_{WA} versus time.

● **Writing a sentence via eye movements:** All the intervening subjects employ computers more than 6 hours per day, this facilitating the execution of the task, and everyone writes the sentence "me gusta viajar" in less than 4 minutes except AW who cannot write it because of her emotional state (anxiety) and calibration problems (mentioned above).

5. CONCLUSIONS

We develop a table top, low cost (U$S 50) pupillometer-eyetraker termed Blick, frame rate is up to 30 fps, images resolution is 640 × 480 pixels for distances eye-sensor around 20 cm and the errors in pupil diameter and gaze direction determinations are 0.05 mm and 1° respectively. The software is programmed in C++ using OpenCV and cvblob libraries and supplies plots, tables and a rendered video of the eye in real time. The hardware comprises an illumination system (two infrared LEDs) and a detection system (lens system of 16mm focal length, filter transmitting only NIR and sensor taken from the Phillips SPC530 camera). It is interesting to point out that the software can operate with other USB cameras having high frame rate, sensibility to NIR and a lens system allowing adequate capture of ocular images.

To exemplify the use of Blick, we consider 6 young healthy subjects (MM, AW, AM, HG, OM and PG) who perform 4 tasks though, prior to this, a pixel-mm calibration (required to precisely measure pupil diameter in millimeters) is carried out for each subject. The first task is to execute, with fixed chin and forehead, a homographic calibration (required to determine gaze direction) and we attain satisfactory results for every subject except AW who moves during and after calibration. Then, each subject´s task is to recognize errors in a set of 4 poker cards (2 of them mistaken), the set being repeated 3 times and each card being presented during 200 ms. We obtain that only the subjects who play with poker cards in daily life (MM and AM) find the errors and, averaging the measurements of the 3 series, for AM alone, we evidence slight pupil dilations of approximately 0.2 mm when each card appears and a dilation increment of 0.05 mm for the mistaken cards. Afterwards each subject has to recognize 2 letters F placed among letters E (this image lasting 30 s). All the subjects identify both letters F and, calculating the difference between the measured pupil diameter and the moving average of this diameter, we obtain that subject PG has the largest pupil dilation when recognizing the letters F, this being approximately 0.04 mm which is of the magnitude order of the measurement error and of values found by other researchers. Finally, all the subjects except AW (whose calibration is inadequate) write a short sentence using Blick as eye tracker and the tool Dasher as interpreter.

Though a largest population would be required to attain more conclusive data, our results suggest that Blick yields pupil diameter and gaze direction adequately and we hope it to be useful in various research areas (Ophthalmology, Physiology, Psychology, etc.) and, also, in helping physically handicapped persons to communicate via eye movements.

ACKNOWLEDGEMENTS

REFERENCES

[1] Kaufman, P. L. and Alm, A., [Adler Fisiologia del ojo], Elsevier, London & New York (2003).

[2] Steinhauer, S. R., Siegle, G. J.; Condray, R. and Pless, M., "Sympathetic and parasympathetic innervation of pupillary dilation during sustained processing", International J. of Psychophysiology 52(1), doi: 10.1016/j.ijpsycho.2003.12.005, 77–86 (2004).

[3] Born, M. and Wolf, E., [Principles of Optics: electromagnetic theory of propagation, interference and diffraction of light], Pergamon Press, Oxford (1980).

[4] Salz, J. J. and Trattler, W., "Pupil size and corneal laser surgery", Current Opinion in Ophthalmology 17(4), 373–379 (2006).

[5] Comastri, S. A., Perez, L. I., Pérez, G. D., Bastida, K. and Martin, G., "Wavefront aberrations: analytical method to convert Zernike coefficients from a pupil to a scaled arbitrarily decentered one", AIP Conference Proc. 992, 69 (2008).

[6] Applegate, R. A., Hilmantel, G., Howland, H. C., Tu, E. Y., Starck, T. and Zayac, E. J., "Corneal first surface optical aberrations and visual performance", J. Refract. Surg. 16(5), 507–514 (2000).

[7] Comastri, S. A., Martin, G. and Pfortner, T., "Analysis of pupil and corneal wavefront aberration data supplied by the SN CT 1000 topography system", Optik 17(11), 537–545 (2006).

[8] Thibos, L. N., Applegate, R. A., Howland, H. C., Williams, D. R., Artal, P., Navarro, R., Campbell, M. C.; Greivenkamp, J. E., Schwiegerling, J. T., Burns, S. A., Atchinson, D. A., Smith, G. and Sarver, E. J., "A VSIA-sponsored effort to develop methods and standards for the comparison of the wave-front aberration structure of the eye between devices and laboratories", Vis. Sci. and Appl. 1, OSA Technical Digest Series, 236-39 (1999).

[9] Marcos, S., "Aberrations and visual performance following standard laser vision correction", J. Refract. Surg. 17, S596–S601 (2001).

[10] Fernández, E. J. and Artal, P., "Ocular aberrations up to the infrared range: from 632.8 to 1070 nm", Opt. Express 16(26), 21199–21208 (2008).

[11] Guell, J. L., Pujol, J., Arjona, M., Diaz-Douton, F., Luque, S. O. and Artal, P., "Objective Optical Quality After Penetrating Keratoplasty and Deep Anterior Lamelar Keratoplasty", Invest. Ophthalmol. Vis. Sci. 46(5), 2712 (2005).

[12] Comastri, S. A., Echarri, R. M. and Pfortner, T., "Correlation between visual acuity and pupil size", Proc. SPIE 5622, 1341–1346 (2004).

[13] Colombo, E. M., L. A., Issolio, Santillán, J. E. and Aguirre, R. C., "Sistema y Procedimiento para la Medición de Funciones Visuales en Seres Humanos". patente Nº 050101283, Argentina (2005).

[14] Pérez, G. M., Manzanera, S. and Artal, P., "Impact of scattering and spherical aberration in contrast sensitivity", J. of Vision 9(3), (2009).

[15] Issolio, L. A., Barrionuevo, P. A., Comastri, S. A. and Colombo, E. M., "Veiling luminance as a descriptor of brightness reduction caused by transient glare", J. Opt. Soc. Am. A 29(10), doi: 10.1364/JOSAA.29.002230. http://josaa.osa.org/abstract.cfm?URI=josaa-29-10-2230, 2230–2236 (2012).

[16] Critchley, H. D., "Emotion and its disorders", British Medical Bulletin 65, doi: 10.1093/bmb/ldg65.035, http://dx.doi.org/10.1093/bmb/ldg65.035, 35–47 (2003).

[17] Klingner, J. M., [Measuring cognitive load during visual tasks by combining pupillometry and eye tracking]. Phd Thesis, Department of Computer Science, Stanford University (2010).

[18] Bijleveld, E., Custers, R. and Aarts, H., "The Unconscious Eye Opener", Psychological Science 20(11), doi: 10.1111/j.1467-9280.2009.02443.x, http://pss.sagepub.com/content/20/11/1313.short, 1313–1315 (2009).

[19] Hess, E. H. and Polt, J. M., "Pupil Size as Related to Interest Value of Visual Stimuli", Science 132(3423), doi: 10.1126/science.132.3423.349, 349–350 (1960).

[20] Partala, T. and Surakka, V., "Pupil size variation as an indication of affective processing", Int. J. of Human-Computer Studies 59, doi: 10.1016/S1071-5819(03)00017-X, http://www.sciencedirect.com/science/article/pii/S107158190300017X, 185–198 (2003).

[21] Rieger, G. and Savin-Williams, R. C., "The Eyes Have It: Sex and Sexual Orientation Differences in Pupil Dilation Patterns", PLoS ONE 7(8), doi:10.1371/journal.pone.0040256, http://dx.doi.org/10.1371%2Fjournal.pone.0040256 , e40256 (2012).

[22] Beatty, J. and Lucero-Wagoner, B., [The pupillary system], Cambridge University Press, Cambridge (2000).

[23] Duchowski, A., [Eye Tracking Methodology, Theory and Practice], 2nd Edition. Springer, New York (2008).

[24] Hess, E.H. and Polt, J.M., "Pupil size in relation to mental activity during simple problem solving", Science 143(3611), doi: 10.1126/science.143.3611.1190, 1190–1192 (1964).

[25] Kahneman, D. and Beatty, J., "Pupil diameter and load on memory", Science 154(3756), doi: 10.1126/science.154.3756.1583, 1583-1585 (1966).

[26] McLaren, J. W., Erie, J. C. and Brubaker, R.F., "Computerized analysis of pupillograms in studies of alertness" Invest. Ophthalmol. & Vis. Sci. 33(3), 671–676 (1992).

[27] Colombo, E., Comastri, S. A., Issolio, L. and Echarri, R., "Pupil light reflex produced by glare under mesopic adaptation", J. of Light & Visual Environment 31(2), doi: 10.2150/jlve.31.70, 70–79 (2007).

[28] Cogain, "Communication by gaze interaction", http://www.cogain.org (2012).

[29] Bianchetti, A., [Determinación del diámetro pupilar ocular en tiempo real], MSc Thesis, Grupo de Óptica y Visión, Departamento de Física, Facultad de Ingeniería, Universidad de Buenos Aires (2012).

[30] Ward, D. J., [Adaptive Computer Interfaces], Phd Thesis, Inference Group, Cavendish Laboratory, Cambridge University (2001).

[31] Bradski, G. and Kaehler, A., [Learning OpenCV], O'Reilly Media Inc. (2008).

[32] González, R. C. and Woods, R.E., [Digital Image Processing], Pearson/Prentice Hall (2008).

[33] Liñan, C. C., "cvBlob libraries", http://cvblob.googlecode.com (2012).

[34] Melkman, A. A., "On-line construction of the convex hull of a simple polyline", Information Processing Letters 25(1), 11–12 (1987).

[35] Williams, T., Kelley, C. and many others, "Gnuplot 4.4: an interactive plotting program", http://gnuplot.sourceforge.net/ (2010).

[36] Karris, S. T., [Introduction to Simulink With Engineering Applications], Orchard Publications, California (2006)